GENERAL ATOMIC

DIVISION OF GENERAL DYNAMICS

GA-4496



# HIGH-TEMPERATURE GAS-COOLED REACTOR CRITICAL EXPERIMENT AND ITS APPLICATION

by

R. G. Bardes, J. R. Brown, M. K. Drake, P. U. Fischer, D. C. Pound, J. B. Sampson, and H. B. Stewart



August, 1963

## DISCLAIMER

**GENERAL ATOMIC**

DIVISION OF

**GENERAL DYNAMICS**

JOHN JAY HOPKINS LABORATORY FOR PURE AND APPLIED SCIENCE

P.O. BOX 608, SAN DIEGO 12, CALIFORNIA

GA-4496

# HIGH-TEMPERATURE GAS-COOLED REACTOR CRITICAL EXPERIMENT AND ITS APPLICATION

by

R. G. Bardes, J. R. Brown, M. K. Drake, P. U. Fischer, D. C. Pound, J. B. Sampson, and H. B. Stewart

This paper is to be presented at the International Atomic Energy Agency Symposium on Exponential and Critical Assemblies in Amsterdam, September 2-6, 1963.

U.S. Atomic Energy Commission
Contract AT(04-3)-314

August, 1963

# I. INTRODUCTION

An important part of the research and development leading to the design of the 40-Mw(e) Peach Bottom High-temperature Gas-cooled Reactor (HTGR) involved the nuclear design and physics evaluation of the reactor. Although much of the information had to be developed from analytical work, some supporting work was required from a critical-experiment program. Because of the kind of information which was needed for the nuclear-design effort, both the type of critical experiment and the experimental program were, perhaps, somewhat unusual. In order to supply basic information on the resonance-absorption characteristics of thorium, the Doppler coefficient of thorium, control-rod effectiveness, and certain lattice parameters, a lattice-cell experiment was utilized. In addition, as a later part of the program, a small-scale, clean-geometry critical experiment was assembled in order to observe the accuracy of the nuclear-design calculational techniques and cross-section data used in calculating physics parameters for semihomogeneous, graphite-moderated reactors with $U^{235}$ as the fuel and thorium as the fertile material.

Two relatively new experimental techniques were developed for measuring resonance integrals and Doppler coefficients in the lattice assembly. These were (1) a reactivity oscillation technique for evaluating thorium Doppler coefficients and (2) an activation technique for determining both the resonance integral of thorium dispersed in graphite and its temperature dependence. Doppler coefficients for fuel elements containing several different thorium concentrations were measured by oscillating cold and hot fuel elements having otherwise identical characteristics in the central region of the test-lattice cell. Comparison of results with theory for the range of conditions examined showed excellent agreement.

The activation measurement of the thorium resonance integral and its

temperature dependence made use of the fact that vanadium is approximately a 1/v absorber and could be used to evaluate the 1/v part of the thorium activation, which was then subtracted from the total thorium activation to obtain the activation resonance integral. This technique was necessary because of the fact that the thorium in the HTGR fuel element is dispersed in graphite, making the usual cadmium-ratio technique difficult to apply. Comparison of experimental and theoretical results showed excellent agreement in the range of variables tested. In addition, the results of both activation and reactivity measurements of Doppler coefficient were in agreement, a fact which is felt to be significant in view of disagreements in results reported by previous investigators. [1]

Experiments on the small clean-geometry assembly were used to test calculational procedures for evaluating over-all temperature coefficients. Reactivity-coefficient measurements afforded a method of checking cross-section data.

## II. PHILOSOPHY OF THE HTGR CRITICAL-EXPERIMENT PROGRAM

The 40-Mw(e) Peach Bottom HTGR employs a graphite moderator and semihomogeneous fuel elements to achieve the following characteristics: high temperatures, high thermal efficiencies, long fuel-burnup times, and good neutron efficiency. The reactor core, which is 7-1/2 ft long and approximately 9 ft in diameter, is made up of 804 fuel elements. The 3-1/2-in. OD fuel elements are composed of a central graphite spine surrounded by an annular fuel body, which in turn is enclosed in a graphite tube. The fuel bodies, which contain approximately one-third of all the graphite in the core, consist of a dispersion of enriched $U^{235}$ and thorium in graphite, the average carbon/thorium/$U^{235}$ atom ratio being 1824/6.7/1.0.

Because of the objectives of the reactor and its design details, the evaluation of some of the reactor physics characteristics involves some very sophisticated analytical procedures. For example, the average graphite temperature in the core is approximately 1200°K, while the reflector graphite temperature is approximately 600°K. Because of the heavy fuel loading in the core and the higher moderator temperature, the cold neutrons which are returned by the reflector have a relatively short diffusion length in the core graphite, thereby creating a strong power peak at the core-reflector interface. This effect is difficult to simulate correctly in a critical experiment and is also difficult to evaluate from few-group diffusion-theory calculations.

Additionally, the HTGR has as a design objective a long fuel residence time and, therefore, a large fuel burnup fraction. In the Peach Bottom reactor it is expected that the average fuel burnup will be approximately 0.6 fissions/initial fissile atom. Because of the large fuel burnup and the production of $U^{233}$ fuel, the characteristics of the core will change appreciably during its burnup history.

Finally, because of the fact that approximately one-third of the moderator is intimately mixed with the fuel, a large part of the moderator temperature coefficient will be prompt, and its contribution to the over-all power coefficient will be very important. The moderator coefficient and the Doppler coefficient of thorium are the only two important contributors to the temperature-coefficient characteristics of the reactor. Furthermore, the temperature-coefficient characteristics change quite radically with fuel burnup owing to the fact that the variation of the $U^{233}$ cross section with energy in the neighborhood of 1 ev is quite different from that of the $U^{235}$ cross section. Since a small fraction of the thermal neutrons falls in this energy range at operating temperatures, the temperature coefficient and therefore the kinetic characteristics of the reactor change throughout the reactor lifetime.

From the previous discussion it can be seen that some of the important physics characteristics are related to high-temperature operation and neutronic changes that occur throughout the operating histroy of the reactor. For this reason, it appeared that the experimental data available from a full-scale critical experiment would not be adequate to specify the nuclear design of the HTGR. Therefore, a detailed analytical program was undertaken to develop methods for calculating in great detail the neutron reaction rates in various parts of the reactor core, taking into account the change in neutron spectrum from point to point throughout the reactor core and reflector. In addition, methods were developed for calculating the changes in core composition and the changes in reaction rates throughout the reactor operating history. Thus, the important problems which were presented to the experimental physicists were related to the adequacy of theoretical calculational techniques and data to be used in the calculations.

As one result of the above considerations, it was concluded that a critical-experiment program should be undertaken to measure reaction rates and the temperature derivatives of these reaction rates in an HTGR lattice. Although the detailed temperature characteristics of the HTGR

could not be duplicated in the critical experiments, the calculational methods and data could nevertheless be checked by experiments covering a fairly broad range of temperatures and compositions. On the basis of the agreement or lack of agreement between experiment and calculations, the areas where differential cross-section data and calculational techniques might be inadequate could then be identified. In some cases where conflicting results occurred, the experimental data might even assist in the correct choice of the best differential cross sections. As a result of the above reasoning, it was also concluded that some experiments on an HTGR-type, small-scale critical assembly should be performed to test the over-all calculational techniques and cross-section data.

Two types of critical experiments were therefore conducted in support of the HTGR nuclear-design program. The first was the test-lattice experiment [2], where detailed measurements of reaction rates were examined in a lattice having a cold neutron spectrum characteristic of the HTGR. This program provided a method for checking the resonance integral of thorium, the Doppler coefficient of thorium, the detailed flux distribution in the lattice, and control-rod effectiveness within a cell. The second experiment [3] was designed as a gross test of the calculational procedures and data. A small critical experiment having a clean geometry and a composition similar to that of the HTGR was constructed. This assembly had approximately one-sixth the volume of the HTGR core and was surrounded on all sides by a 2-ft graphite reflector. Owing to the small core size and the large reflector area, this experiment provided a severe test of the calculational methods. Experiments with this facility encompassed reactivity-coefficient measurements, neutron-flux distributions, effectiveness of groups of control rods, and a measurement of the over-all temperature coefficient.

## III. HTGR CRITICAL-ASSEMBLY FACILITY

A general view of the HTGR critical assembly is shown in Fig. 1. The assembly was built in two halves so that it could be separated at the mid-plane. Gross control of the reactor was achieved by the separation of the two halves, and fine control was accomplished by means of control rods that could be driven into the active lattice region. Figure 2 shows typical fuel elements used in the critical assembly. Most of the fuel elements consisted of rectangular graphite blocks containing fuel compacts inserted in two parallel holes. Compacts of either $U^{235}$ and graphite or thorium and graphite could be loaded into the blocks to achieve the composition desired. At the right of the figure are the parts of an HTGR mock-up fuel element used in the central lattice-cell region of the test-lattice reactor. Included in the figure are the graphite sleeve, an annular fuel body, and a section of the graphite spine.

Figure 3 shows the face of one of the halves of the 6 ft-long test-lattice reactor. The 16-in.-diameter test-lattice cell, consisting of a hexagonal array of 19 HTGR fuel elements, is shown at the center of the assembly. Reactivity measurements were obtained in the central fuel-element position of the lattice cell. Figure 4 is a schematic drawing of the assembly. The 19 cylindrical fuel elements at the center of the reactor had essentially the same material composition and dimensions as the fuel elements in the Peach Bottom HTGR. This test-cell region was surrounded by a buffer-lattice region roughly 3 ft square consisting of critical-assembly fuel blocks containing $U^{235}$ and thorium. The composition of the buffer region was chosen such that the reaction rates in the region were approximately the same as those in the test-lattice region. The loading was adjusted by means of boron–stainless steel poison strips to obtain a convenient amount of excess reactivity and to achieve a flat neutron flux over

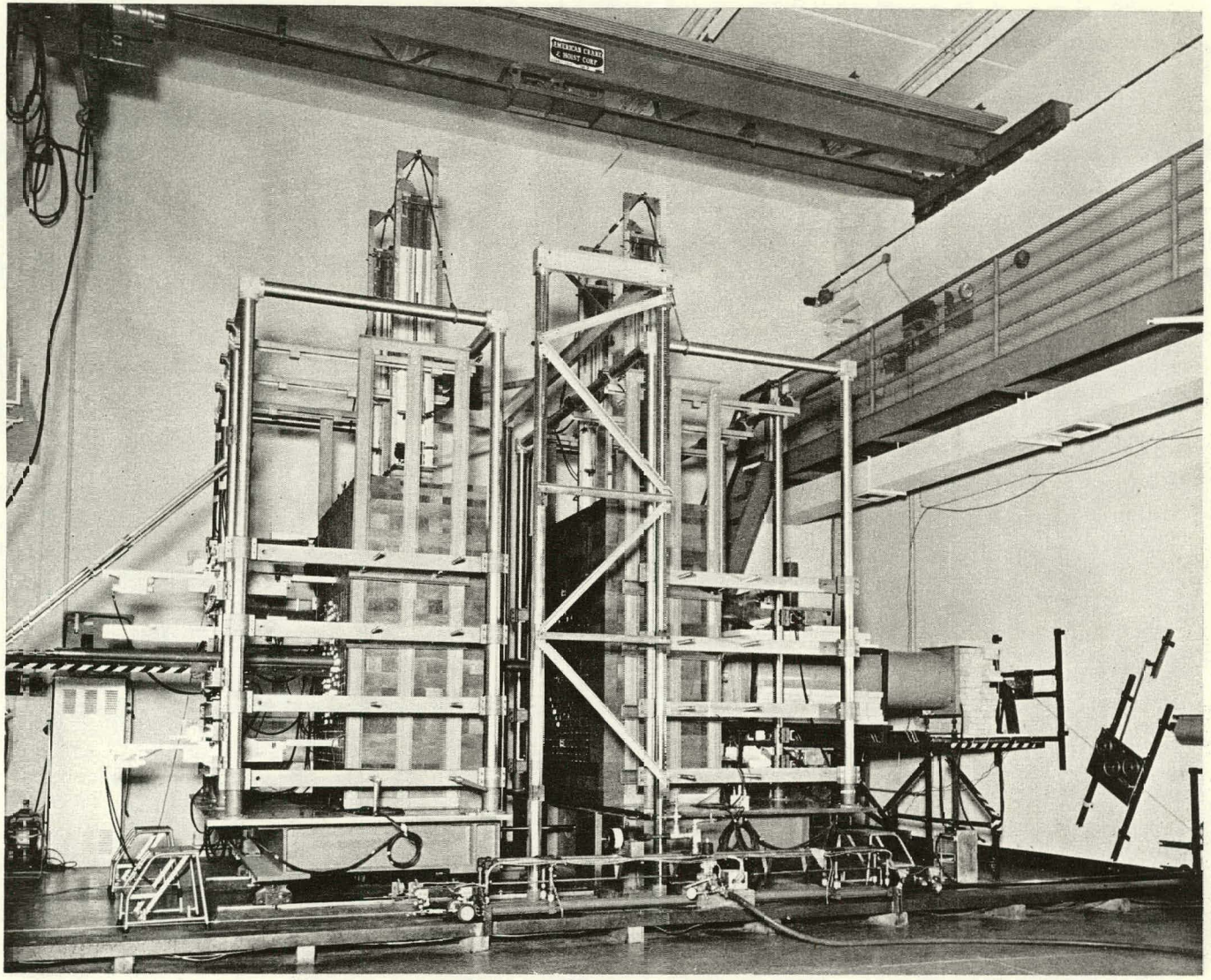

Fig. 1--Over-all view of Peach Bottom HTGR critical assembly

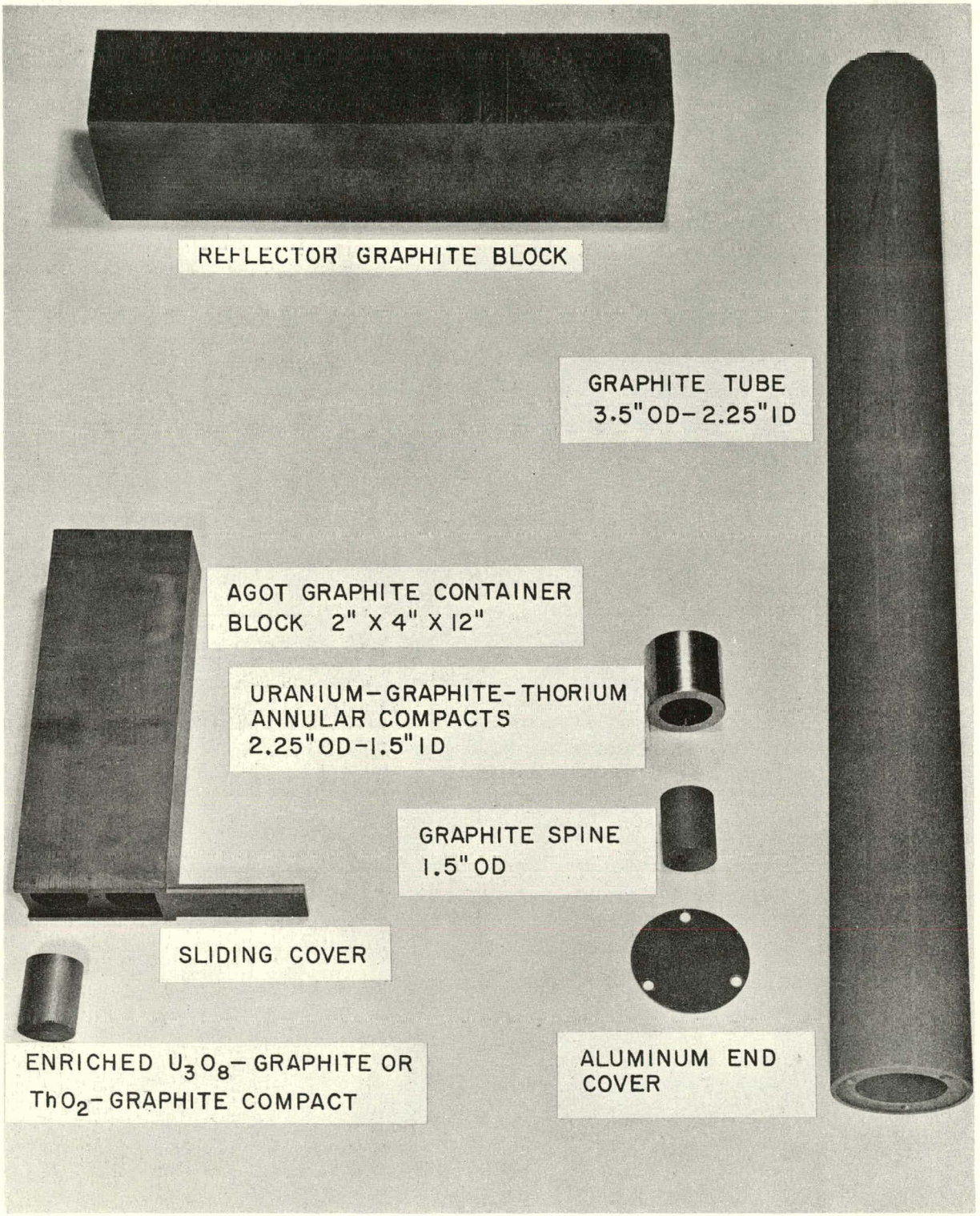


Fig. 2--Fuel elements used in HTGR critical assembly

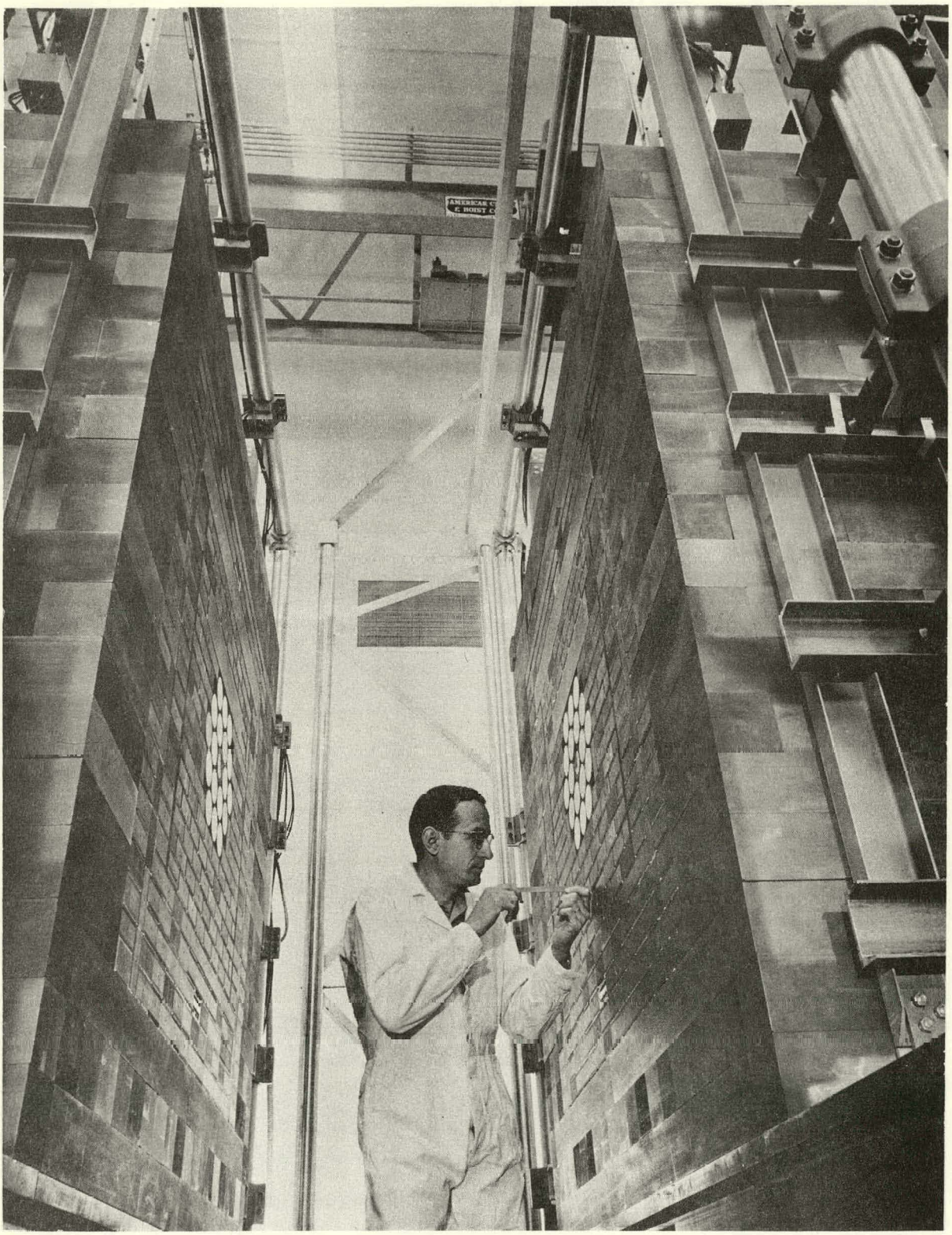

Fig. 3--Peach Bottom HTGR critical assembly; view at plane of separation

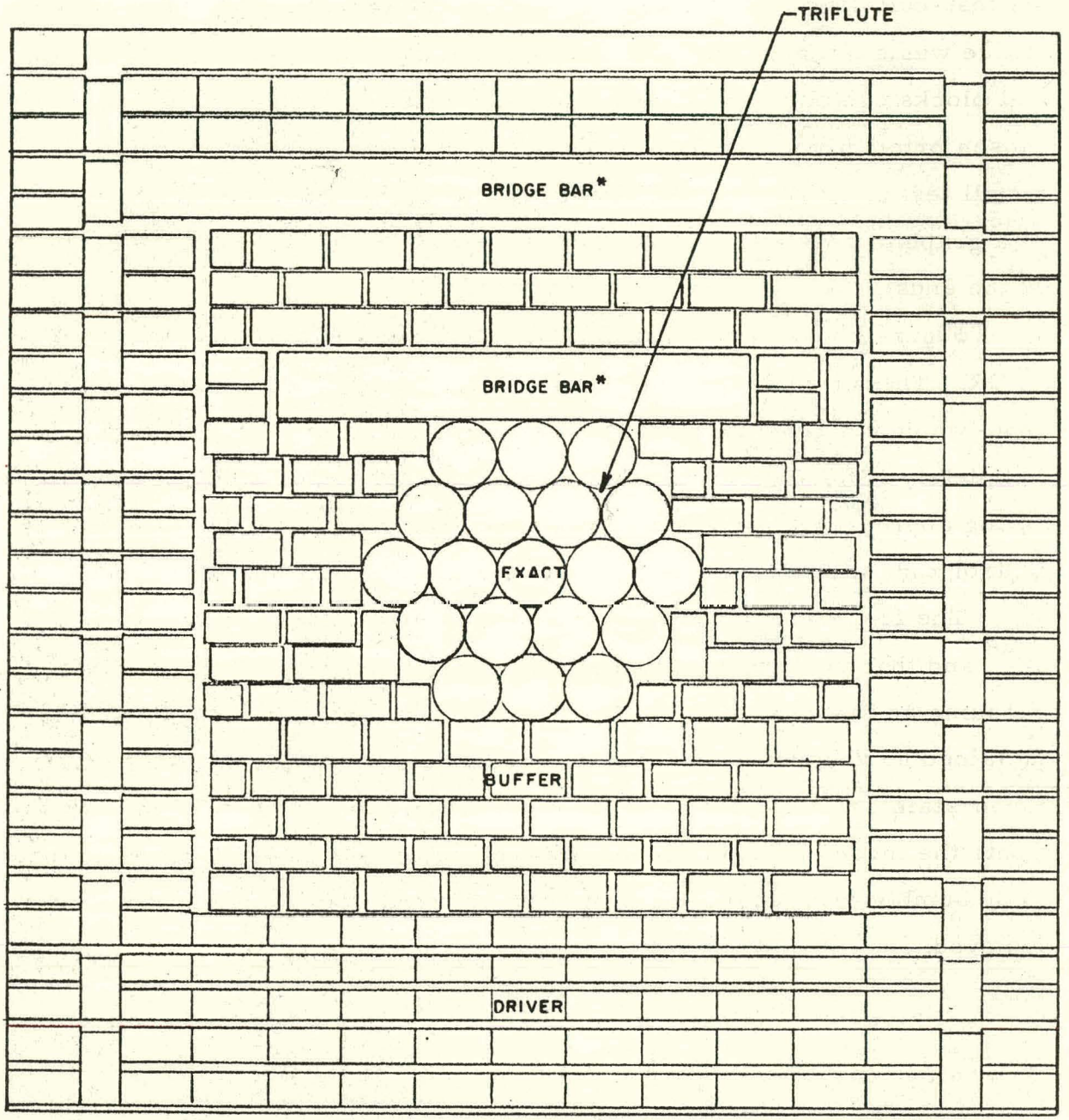


* BRIDGE BARS ARE LOADED WITH THE SAME CONCENTRATION OF URANIUM AND THORIUM AS THE SURROUNDING REGIONS.

APPROXIMATE SCALE: 1 TO 9

Fig. 4--Core cross section in the transverse plane perpendicular to the axis of symmetry (the reflector is not shown; the bridge bars are made of the same material as the adjacent blocks of the region)

the test-cell diameter and much of the buffer-lattice region. The buffer lattice was surrounded by a driver lattice ~10 in. thick and consisting of fuel blocks containing $U^{235}$ and graphite. The $U^{235}$ composition was chosen primarily to assure that the entire assembly could be made critical for all test programs contemplated. The driver lattice was surrounded by a graphite reflector ~1 ft thick (the critical assembly was unreflected on the ends).

Figure 5 is a view of the face of the one-sixth-scale mock-up of the HTGR. The mock-up assembly had a core about 5 ft in diameter and 4 ft long, which could be separated at the vertical mid-plane. The core was completely reflected by about 2 ft of graphite and contained 19 square holes having approximately the same fractional void volume as that required for control rods in the Peach Bottom HTGR.

The fuel elements were all rectangular fuel blocks containing both $U^{235}$ and thorium, the carbon/thorium/$U^{235}$ atom ratio being approximately the same as that specified for the Peach Bottom reactor. The assembly contained no rhodium poison or boron burnable poison but did have some boron—stainless steel strips to shim the reactivity. In most of the experiments the inventory of the boron—stainless steel strips was chosen so that the assembly was just critical at room temperature with all control rods removed.

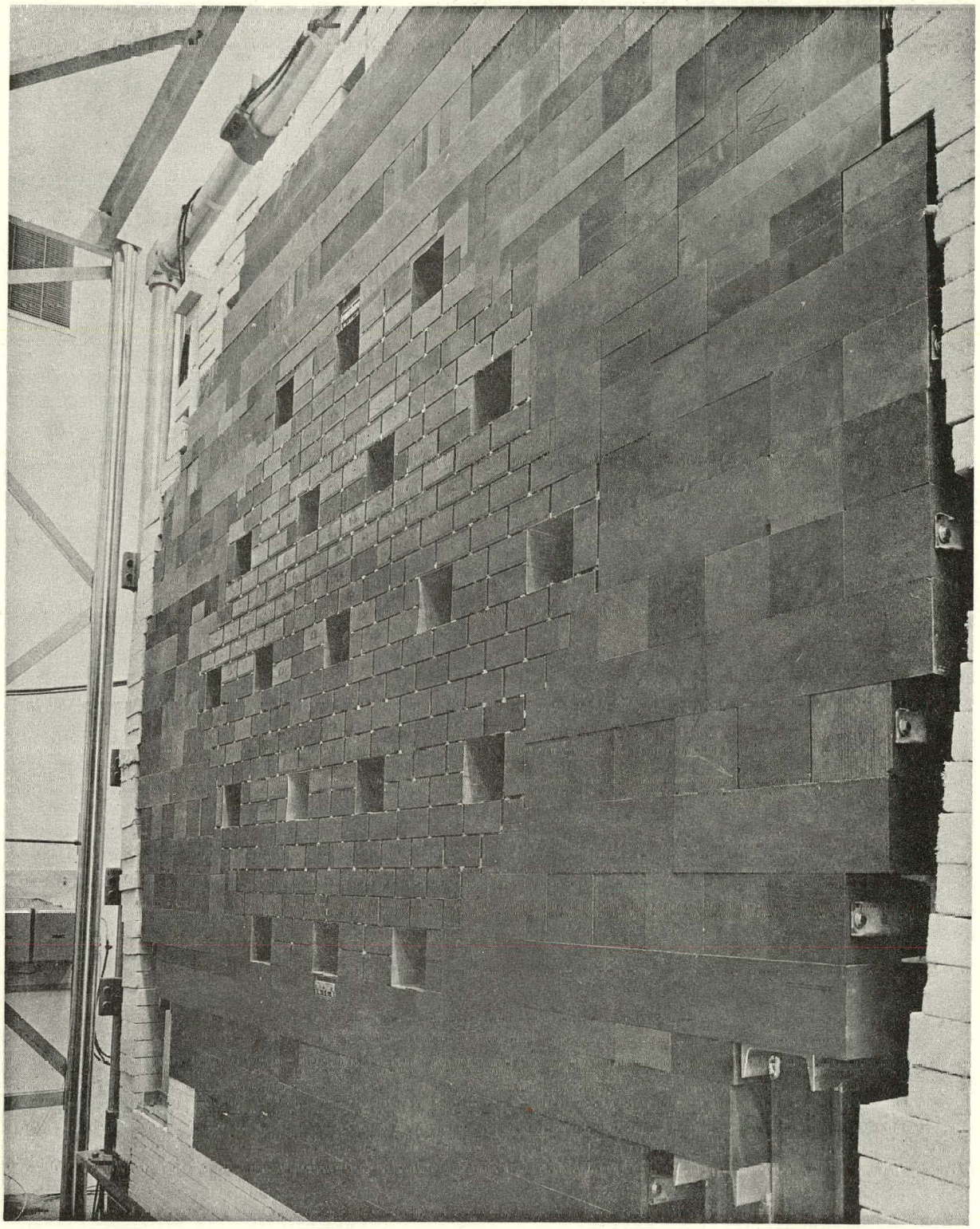

Fig. 5--Critical assembly used for the experimental program; view at plane of separation

## IV. CRITICAL-EXPERIMENT MEASUREMENTS IN THE TEST-LATTICE ASSEMBLY

In this section, the utility of the test-lattice assembly will be illustrated by reviewing some of the important experiments which were performed during the first part of the HTGR critical-assembly program. In particular, the activation measurements leading to the evaluation of the thorium resonance integral will be described. The measurement of the Doppler coefficient by pile oscillator and activation techniques will also be described.

Until 1962 the differential cross-section data that were available for thorium [4] led to an infinitely dilute resonance integral of 96 barns. Resonance-integral measurements [5] indicated values ranging from 60 to 110 barns. Clearly, more definitive experimental information was required to check the differential data and resolve the discrepancies in the integral measurements. Experiments were therefore undertaken to measure the thorium resonance integral under the following conditions:

1. Infinitely dilute sample, 1/E spectrum.
2. Infinitely dilute sample, HTGR spectrum.
3. HTGR composition and geometry, HTGR spectrum.

The usual activation technique, involving the irradiation of cadmium-covered samples, was difficult to apply to the HTGR measurements, since the HTGR fuel element contains moderator material intimately mixed with thorium. Therefore, an alternative technique was developed which involved activation measurements of both thorium and vanadium. Previous measurements [6] on vanadium had shown that it is very nearly a 1/v absorber and leads to a radioactive isotope having a convenient half life of 3.77 min. Hence, by renormalizing the vanadium absorption rate to that of an isotope having the same thermal absorption cross section as thorium, the 1/v

absorption rate of thorium arising from the epithermal flux could be evaluated and subtracted from the over-all thorium absorption rate--leading to the resonance-absorption component for the thorium sample. This procedure was identified as the vanadium-subtraction technique. [7]

The relative absorption rates for thorium and vanadium were determined by activation measurements in a well-thermalized, Maxwellian flux obtained in the thermal column of the TRIGA Mark F reactor [8] at General Atomic. The relative absorption rates for the two samples could be calculated quite accurately for this condition, since the thermal-neutron absorption cross sections are well known for the two nuclides.

A similar calibration was carried out for some standard gold foils so that the thorium resonance integral could be measured relative to that of gold, which is well known. The resonance activation of the gold and the thorium were then measured in a particular region of the General Atomic TRIGA Mark F reactor where the epithermal flux was calculated to be approximately $1/E$.

The spectrum appropriate to the Peach Bottom HTGR was developed in the central lattice region of the HTGR critical assembly. Two types of fuel geometries, annular and cylindrical, were used in the measurements. The measurements made in the annular geometry were of primary interest because that configuration corresponded to the design geometry of the Peach Bottom HTGR. Measurements were also made in thorium-graphite cylindrical pellets corresponding to the pellets used in the buffer region of the test-lattice reactor.

In most cases, thin metallic foils were used in the activation determination. However, in some cases the activation of the thorium within the thorium-graphite compact was directly determined. Major factors in making quantitative measurements of resonance absorption are the type, size, geometry, thickness, and preparation of the various foils. There were two important factors to be considered in the foil selection. First, the foils had to be sufficiently thin so that there would be practically no

self-shielding effect in the resonance-energy region, but sufficiently thick so that they could be handled. Second, there had to be a uniform distribution of material throughout the foils so that any small amount of self-shielding that was present would be constant. Table I gives typical characteristics of the thin foils employed.

The foil position, in relation to the medium in which the activation was being made, was very important in the HTGR spectrum measurements. In most cases, the geometry of the thorium-containing region was a cylindrical annulus. Pie-shaped foils, as shown in Fig. 6, were used to average correctly the radial variation of the activation rate over a sector of the annulus. Each foil covered one-sixth of the cross-sectional area of the annulus. Two sets of thorium, gold, and vanadium foils were used in reactor positions having the same flux environment.

Figure 7 shows the detailed arrangement of the foils in the compacts. It was important to eliminate gaps between the compacts to prevent any streaming down the foil-compact interface. The uranium was omitted from the compacts adjacent to the thorium foil in order to avoid contaminating the foils with fission-product activity. The perturbation caused by omitting the uranium in this compact was shown to be a 1% correction in the measured resonance reaction rates, since the flux dip caused by the uranium was less than a few percent and was mostly thermal. The thorium foils were positioned between the two thorium-graphite compacts. The vanadium and gold foils were positioned between one of the thorium-graphite compacts and the thorium-uranium-graphite compact. These foils were enclosed in aluminum foil to prevent them from becoming contaminated from either activated thorium or uranium fission products. This assembly of foils and compacts then became part of the loaded central fuel element of the test-lattice region.

The foils activated in the TRIGA thermal column were arranged so as to duplicate, as nearly as possible, the activation assembly in the test-lattice region. To ensure that each part of the activation assembly

Table I

FOIL CHARACTERISTICS

| Material | $\sigma_{2200}$ m/sec (barns) | Thickness ($mg/cm^2$) |
|---|---|---|
| $Au^{197}$ | 98.86 | 0.17 |
| Vanadium | 4.5 | 7.6 |
| $Th^{232}$ | 7.45 | 3.3 |

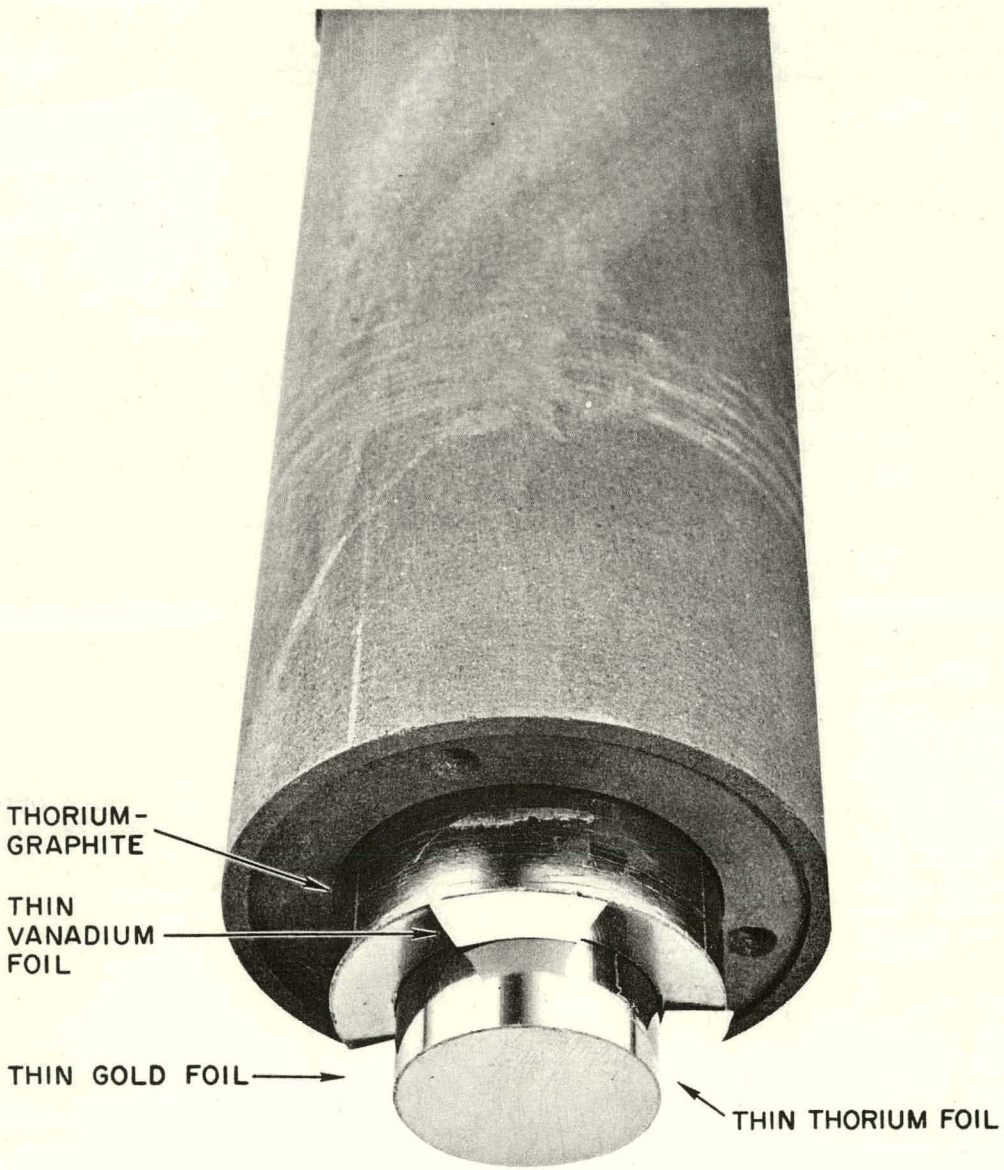


Fig. 6--Foils partially assembled in HTGR-type fuel compacts

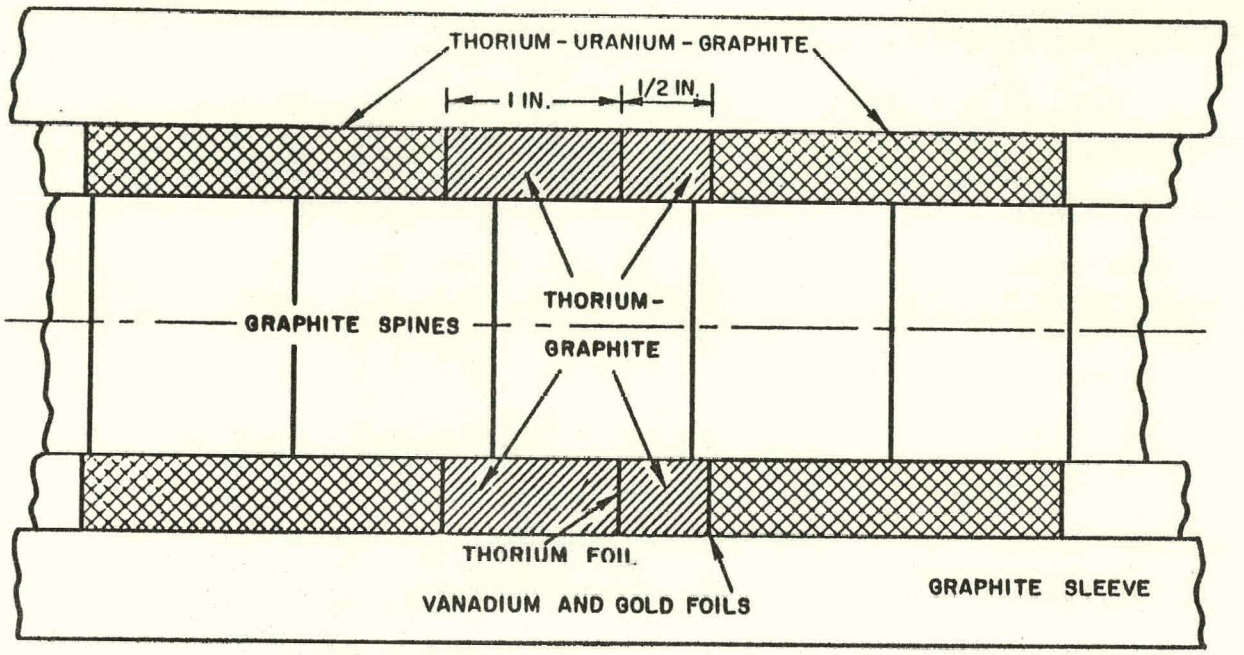


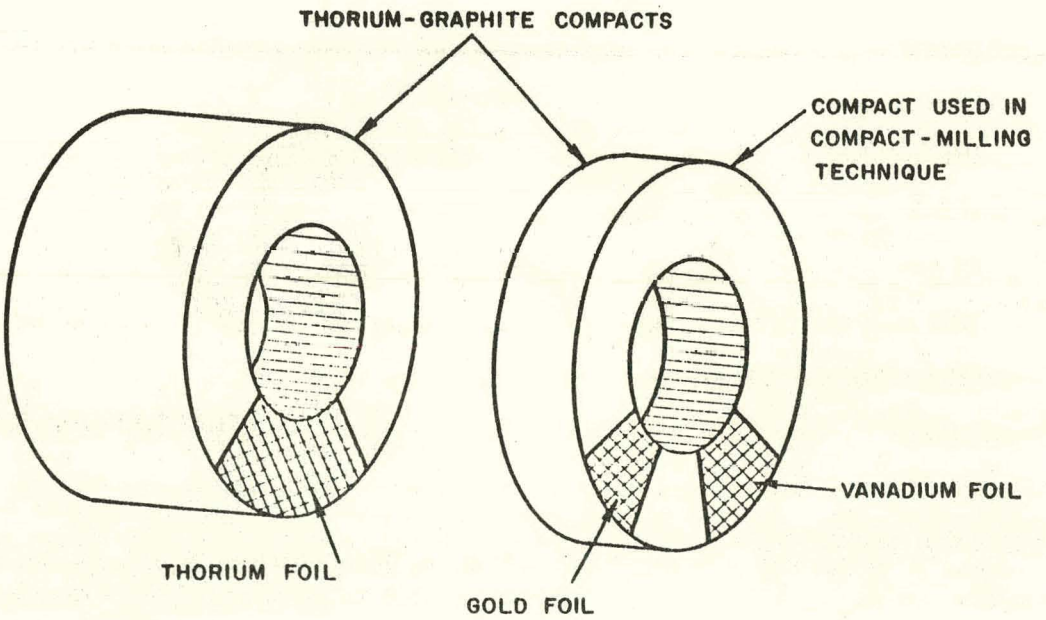


Fig. 7--Foil and compact arrangement for resonance integral measurements

received the same exposure, the assembly was positioned on a small turntable driven by a 30-rpm motor.

The 1/E spectrum measurements were made by activating foil detectors inside a hollow dummy element in the TRIGA Mark F reactor. The foils were positioned along the centerline of a dummy element at the vertical midplane of the core adjacent to the reflector. Three sets of foils were used, each set being composed of one of each type of foil (gold, vanadium, and thorium). The foils were again separated by aluminum spacers to prevent cross contamination and were packaged in aluminum foil. Duplicate sets of foils were exposed in the thermal column. The foil packages for the thermal-column exposure were positioned on the rotating turntable for the irradiation.

Several factors had to be considered in selecting the length of irradiation time and the power level at which the irradiations were to be made. These factors were primarily associated with obtaining sufficient activation of the materials involved so that good counting statistics could be obtained. To eliminate any errors associated with counting-equipment drift or foil decay uncertainties, two activations were made simultaneously, i. e., the activation in the spectrum of interest and the activation in the Maxwellian spectrum.

In the case of the HTGR spectrum measurements, both the critical assembly and the TRIGA Mark F reactor (with thermal column) were involved. The simultaneous start-up and shutdown of these facilities was accomplished by means of telephonic communications. The uncertainty in absolute time between the shutdown time of the two reactors was of the order of 1 sec or less. This uncertainty was insignificant compared with the shortest half life of any of the detector foils (vanadium, with a half life of 225 sec). In both reactors the relative power level was maintained constant to better than 0. 1% during the irradiations.

When the foils were removed from their respective irradiation positions, the most important factor was to minimize the delay in starting

to count the 225-sec half-life activity of the vanadium foils. The foils of a particular material from both irradiations were counted concurrently, e. g., the vanadium foils from the critical assembly were counted at the same time as the vanadium foils from the thermal column. This system of counting eliminated possible errors in decay corrections or drifts in the counting equipment.

Two separate counting systems were used to measure the induced activity of the foils. The beta activity of the 22-min $Th^{233}$ was measured with a gas-flow proportional counter. The gamma activity of the vanadium and the gold (0. 4-Mev gamma-emission line) was measured using a 1-1/2-in. NaI(Tl) well-type scintillation crystal.

A separate and independent method for measuring the activation rates of thorium was also developed. This method was based on the direct measurement of the activation rate of thorium dispersed in a thorium-graphite compact. Basically, the method involved the activation of a thorium-graphite compact, together with foils of vanadium and gold, in both the critical assembly and the TRIGA thermal column, as described previously. This method was used as a supplement to foil measurements, and in all cases where it was applied thorium foil detectors were also used. The gold and vanadium activations were used in the interpretation of both the foil and compact activations.

This method involved a milling device, as shown in Fig. 8. The irradiated compact was clamped to the center of a simple milling head that could be slowly rotated by a motor-driven worm-gear drive. A small, high-speed milling tool was positioned to cut the flat end of the compact. As the motor slowly (2 rpm) rotated the compact, the high-speed milling tool cut a thin layer from the compact surface. The thorium-graphite powder removed in the cutting was collected on a filter paper, which was inserted into a holder in a short suction tube. From this point on, the collected sample was treated basically the same as the foil detectors.

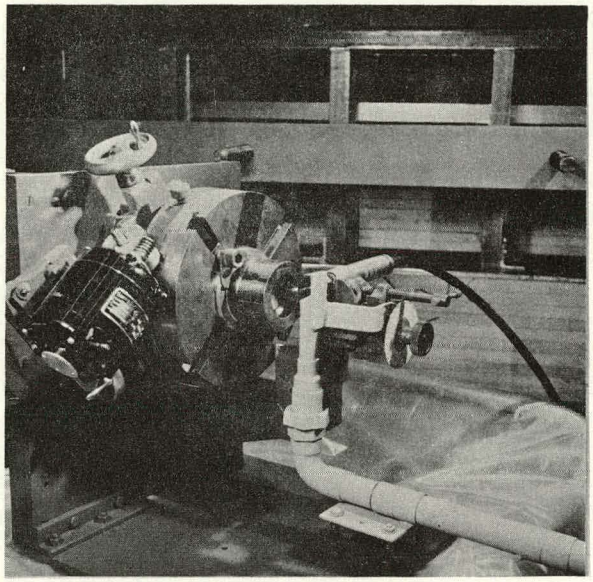

Fig. 8--Compact-milling equipment

The significant point about this method of measurement is that the activation detector was essentially the same material as that for which the resonance absorption rate was being studied.

The measured activities, as obtained from the two counting systems, were corrected for weights and decay times in the usual manner. From the appropriate activation ratios for vanadium, gold, and thorium, it was possible to calculate the resonance integral for thorium in a particular spectrum. The basic principle behind the vanadium-subtraction method and detailed results obtained with it have been described by Sampson.[9] Table II summarizes the results of these measurements for several geometric configurations and thorium loadings.

It is noted that the experiments led to an infinitely dilute resonance integral of 79 barns, instead of the 96 barns previously obtained from the differential cross-section data. As a result of this discrepancy, the resonance parameters of thorium in the neighborhood of 20 ev were adjusted to obtain agreement. It can be seen from the comparison of the calculated and measured results that this correction does not lead to good agreement for the other samples. Subsequent differential cross-section measurements [10] and interpretations [11] have been reported, but it appears that additional work on thorium is required.

In addition to the measurements of the thorium resonance integrals, a program was undertaken to measure the temperature response of the resonance integral, or the Doppler coefficient, for various fuel-element compositions and geometries.[12] These Doppler-coefficient measurements were performed primarily by a reactivity oscillation technique, where the reactivity swing resulting from the alternate substitution of a cold and hot fuel element in the test lattice was measured. In addition, activation measurements of the neutron absorption rates in hot and cold thorium samples were made for one particular fuel-element design.

The component of the temperature coefficient of a power reactor arising from the Doppler coefficient can be shown to be [1]

Table II

COMPARISON OF CALCULATED AND MEASURED RESULTS FOR $Th^{232}$ RESONANCE CAPTURES

| System Measured | Measured $I_{eff}$ (barns) | | Calculated $I_{eff}$ (barns) |
|---|---|---|---|
| | Foil Detector | Activated-compact Detector | |
| 1/E spectrum, thin limit | 79.0 | ---- | 79.6 |
| Small fuel annulus | | | |
| C/Th = 55.7 | 35.2 | 37.4 | 34.4 |
| C/Th = 48.7 | 33.4 | 32.7 | 31.7 |
| Large fuel annulus | | | |
| C/Th = 123.8 | 43.7 | 46.0 | 41.5 |
| Buffer cylinder | | | |
| C/Th = 46.8 | 28.3 | ---- | 28.9 |

$$\frac{1}{k}\left(\frac{dk}{dT}\right)_{Doppler} = \frac{1}{p}\frac{dp}{dT} = \alpha \frac{d \ln p}{dT} ,$$

where $\alpha = (1/I)(dI/dT)$ is defined as the Doppler coefficient. It was, then, the magnitude of the Doppler coefficient, $\alpha$, which was the objective of the oscillation experiment in the test-lattice assembly. It can be shown [13] from perturbation theory that the component of the reactivity swing due to the change in thorium absorption rate, i.e., $\Delta \rho_{res}$, is related to the resonance absorption, $I_{eff}$, approximately by

$$\frac{1}{\rho_{res}}\frac{\Delta \rho_{res}}{\Delta T} = \frac{1}{I_{eff}}\frac{\Delta I_{eff}}{\Delta T} .$$

Detailed calculations for the test-lattice assembly showed that the error in this relation would be less than about 1% for cases of interest.

In order to evaluate the Doppler coefficient, it was thus necessary to measure both the incremental change in reactivity, $\Delta \rho_{res}$, resulting from the temperature change, and the total reactivity value, $\rho_{res}$, of the sample. It was, of course, important to obtain only the components of reactivity, $\rho_{res}$, and the reactivity swing, $\Delta\rho_{res}$, which were contributed by the change in the resonance absorption of the thorium.

The reactivity, $\rho_{res}$, was measured simply by observing the difference in reactivity between the thorium-loaded, HTGR-type fuel element and a fuel element containing the same materials, but having the thorium replaced by boron so that the 1/v absorption was the same in both cases. Under these conditions,

$$\rho_{res} = \rho - \rho_{1/v} ,$$

where $\rho$ is the total reactivity effect of the thorium and $\rho_{1/v}$ is the 1/v contribution as deduced from the fuel element containing boron.

The total reactivity swing between the hot and cold fuel elements includes components due to the change in resonance absorption and the 1/v absorption. Furthermore, the presence of the hot graphite moderator

Table II

COMPARISON OF CALCULATED AND MEASURED RESULTS FOR $Th^{232}$ RESONANCE CAPTURES

| System Measured | Measured $I_{eff}$ (barns) | | Calculated $I_{eff}$ (barns) |
|---|---|---|---|
| | Foil Detector | Activated-compact Detector | |
| 1/E spectrum, thin limit | 79.0 | ---- | 79.6 |
| Small fuel annulus | | | |
| C/Th = 55.7 | 35.2 | 37.4 | 34.4 |
| C/Th = 48.7 | 33.4 | 32.7 | 31.7 |
| Large fuel annulus | | | |
| C/Th = 123.8 | 43.7 | 46.0 | 41.5 |
| Buffer cylinder | | | |
| C/Th = 46.8 | 28.3 | ---- | 28.9 |

$$\frac{1}{k}\left(\frac{dk}{dT}\right)_{\text{Doppler}} = \frac{1}{p}\frac{dp}{dT} = \alpha \frac{d \ln p}{dT} ,$$

where $\alpha = (1/I)(dI/dT)$ is defined as the Doppler coefficient. It was, then, the magnitude of the Doppler coefficient, $\alpha$, which was the objective of the oscillation experiment in the test-lattice assembly. It can be shown [13] from perturbation theory that the component of the reactivity swing due to the change in thorium absorption rate, i.e., $\Delta \rho_{res}$, is related to the resonance absorption, $I_{eff}$, approximately by

$$\frac{1}{\rho_{res}}\frac{\Delta \rho_{res}}{\Delta T} = \frac{1}{I_{eff}}\frac{\Delta I_{eff}}{\Delta T} .$$

Detailed calculations for the test-lattice assembly showed that the error in this relation would be less than about 1% for cases of interest.

In order to evaluate the Doppler coefficient, it was thus necessary to measure both the incremental change in reactivity, $\Delta \rho_{res}$, resulting from the temperature change, and the total reactivity value, $\rho_{res}$, of the sample. It was, of course, important to obtain only the components of reactivity, $\rho_{res}$, and the reactivity swing, $\Delta\rho_{res}$, which were contributed by the change in the resonance absorption of the thorium.

The reactivity, $\rho_{res}$, was measured simply by observing the difference in reactivity between the thorium-loaded, HTGR-type fuel element and a fuel element containing the same materials, but having the thorium replaced by boron so that the 1/v absorption was the same in both cases. Under these conditions,

$$\rho_{res} = \rho - \rho_{1/v} ,$$

where $\rho$ is the total reactivity effect of the thorium and $\rho_{1/v}$ is the 1/v contribution as deduced from the fuel element containing boron.

The total reactivity swing between the hot and cold fuel elements includes components due to the change in resonance absorption and the 1/v absorption. Furthermore, the presence of the hot graphite moderator

tends to re-thermalize the neutrons in the immediate neighborhood of the sample and consequently changes the reaction rates of all the thermal absorbers locally. Hence,

$$\Delta \rho = \rho(T) - \rho(T_0) \ ,$$

$$= \rho_{res}(T) + \rho_{th}(T) - \rho_{res}(T_0) - \rho_{th}(T_0) \ ,$$

where T and $T_0$ refer to the hot and cold samples and $\rho_{res}$ and $\rho_{th}$ refer to the reactivity changes arising from changes in resonance absorption and thermal spectrum absorptions, respectively. It is important to remember that the reactivity effect $\rho_{th}$ may include changes both in absorption rates in the sample and absorption rates in surrounding fuel, thorium, and other absorber materials. This is particularly true when the sample is at an elevated temperature relative to the rest of the lattice.

Rewriting the above equation as

$$\Delta \rho = [\rho_{res}(T) - \rho_{res}(T_0)] - [\rho_{th}(T) - \rho_{th}(T_0)] \ ,$$

$$= \Delta \rho_{res} - \Delta \rho_{th} \ ,$$

it is seen that the resonance term can be obtained from the total reactivity swing by subtracting the thermal-base component, $\Delta \rho_{th}$. In order to obtain an accurate value of $\Delta \rho_{res}$, it is therefore necessary to (1) minimize the component $\Delta \rho_{th}$, and (2) evaluate carefully the $\Delta \rho_{th}$, using samples where the thorium is again replaced by an equivalent 1/v absorber.

The physical nature of the thermal-base effect was analyzed theoretically [12], and it was shown that the effect nearly vanishes in a spatially uniform neutron-flux distribution. This can be seen from rather simple considerations. If the fuel and all absorber cross sections have a 1/v variation in the thermal-spectrum region and if the fuel and absorber atoms are all located together relative to neutron-flux variations, and finally if the $k_\infty$ of the lattice is just unity, then a local change in the thermal-neutron spectrum would affect all local reaction rates in the same

way--and therefore the over-all reactivity would be unchanged.

Thus, in order to minimize the thermal-base effect, the radial flux distribution in the assembly was flattened by the introduction of poison in the void space between fuel elements. No attempt was made to flatten the flux in the axial direction. In addition to flattening the radial flux, careful attention was given to the 1/v poison distribution in the sample itself to ascertain that local changes in the neutron flux would not affect reaction rates in the fuel and other absorbers in different ways. By this means, the thermal-base effect was reduced to about 20% of the total reactivity swing.

Since the change in reactivity caused by replacing a cold fuel element with a hot fuel element was typically 0.01 dollar or less, and the sensitivity to which the reactivity differences could be measured was 0.0001 dollar, it was desirable to make repetitive measurements of these reactivity changes to improve the statistical accuracy of the measurement. The method used in these measurements might be more appropriately described as a periodic substitution procedure rather than an oscillation procedure. The purpose was to periodically interchange the hot and cold central fuel tubes and to record the reactivity difference associated with a measured temperature difference.

The oscillator mechanism used for these measurements consisted of a double-acting pneumatic cylinder with a piston with an 8-ft stroke.[12] This device was equipped with hydraulic snubbers which contacted stops at both ends of its travel. By means of stainless steel cables through pulleys attached to the walls of the room, this mechanism moved a 14-ft-long oscillator element horizontally through the core. The oscillated fuel element consisted of two 6-ft-long graphite fuel tubes separated by a 2-ft-long section of Transite (thermal insulation) and coupled to the graphite by threaded aluminum sleeves. All sections of the oscillator sample had a common diameter of 3.57 in. Full travel of the pneumatic cylinder resulted in the exchange of one 6-ft-long fuel tube in the core for the other, an action requiring about 1 sec.

A 6-ft-long cylindrical oven was positioned horizontally at one end of the core so that when one end of the oscillator element (the cold fuel tube) was in the core, the other end (the hot fuel tube) was in the oven. When the hot end was in the core, the cold end rested in a graphite trough situated horizontally off the other end of the core. Figure 9 shows the location of the oven.

A thin air gap and strips of Transite provided sufficient thermal insulation around the hot fuel element so that heat transfer to the surrounding six fuel tubes resulted in a temperature rise of less than $10^{\circ}$F per minute when the hot element was at $800^{\circ}$F. Over a period of several hours, the Transite insulation between the hot and cold fuel tubes was sufficient to limit the temperature rise to less than $10^{\circ}$F at the end of the cold fuel tube. Thermocouples monitored the temperature of the entire 14-ft oscillator element. The temperature distribution over the hot fuel tube of the oscillator element was fairly uniform. In the longitudinal direction, the maximum variation from end to center was about $40^{\circ}$F at the highest temperature ($800^{\circ}$F). The radial distribution was essentially uniform.

During the measurements of the Doppler coefficient, the oscillator mechanism was usually programmed to move every 30 sec, each movement requiring about 1 sec, so that each end of the oscillator element alternately had a dwell time of about 29 sec in the core.

Rather than record the variations of the neutron flux as the oscillator element was moved, the flux level was automatically maintained constant by means of a servo-driven control rod located in the reflector. This servo-rod was a thin boral strip 3 ft long, having a total worth of about 6 cents. The servo-system was actuated by an error signal between the average current output of two ion chambers (gamma-compensated) located in the reflector and a fixed current supply. A servo-amplifier operating at high gain drove the servo-rod positioning motor. The speed of travel of the servo-rod was such that it changed reactivity at the rate of 3 cents per second over the most effective portion of its position.

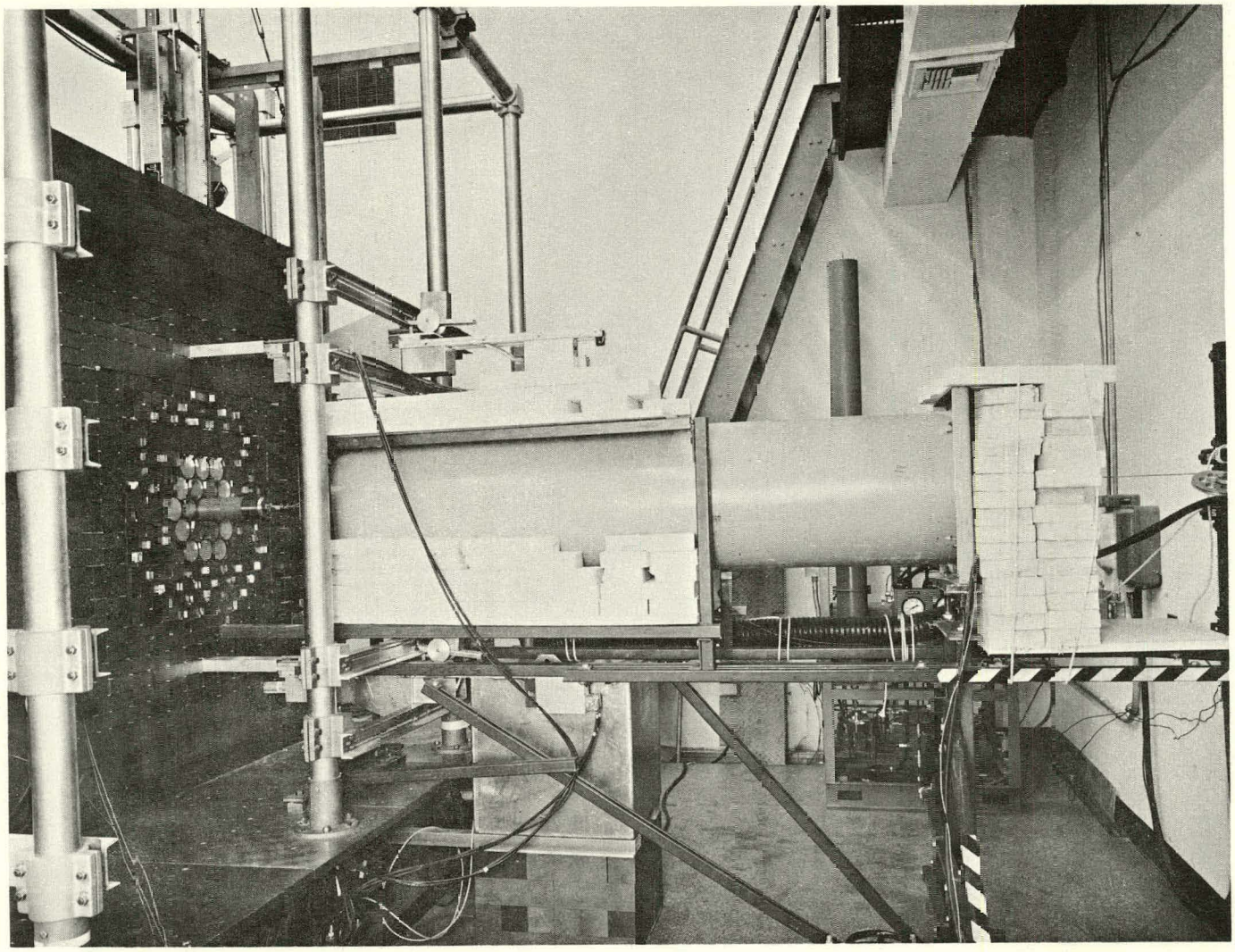

Fig. 9--External oven placement near critical assembly

Doppler-coefficient measurements were made for several thorium loadings and for three different sizes of annuli by the reactivity-swing method. Figures 10 and 11 show, respectively, the dependence of reactivity on temperature and the Doppler coefficient as a function of temperature for three fuel compacts measured. Table III gives the measured and calculated Doppler coefficients averaged over the temperature range 300° to 700°K for several fuel-element compositions.

An over-all experimental uncertainty of ±10% has been estimated for the individual measurements of $(1/I)(dI/dT)$. The uncertainty in the average Doppler coefficient, over the temperature range 300° to 700°K, is probably smaller than ±10%. This estimate of probable accuracy is based partly on statistical uncertainties and partly on observations of the experimental reproducibility.

As a check on the reactivity method of determining the Doppler coefficient, an activation technique was used for one measurement.[12] The result of a direct activation measurement of $(1/I_{eff})(dI_{eff}/dT)$ was $(3.7 \pm 0.8) \times 10^{-4}/^{\circ}C$ averaged over the range 300° to 700°K. This is to be compared with values of $(3.6 \pm 0.4) \times 10^{-4}/^{\circ}C$ and $3.4 \times 10^{-4}/^{\circ}C$, respectively, obtained over the same temperature range for the reactivity oscillation method of measurement and the theoretical determination. The agreement is quite satisfactory and indicates that there are no serious systematic errors in the measurement by the reactivity method.

The activation method of measurement utilized the 1/v subtraction technique that was developed for measurements of the resonance integral of thorium, as previously described. The measurements of the Doppler coefficient were made in a small vacuum-insulated oven at the center of the critical assembly, where temperatures up to 1000°F were obtained. The oven was designed as a thin aluminum shell, 4-3/4 in. long and 3-3/4 in. in outside diameter, to enable it to be located in the central fuel-element position of the test-lattice region. The oven contained a 4-in. length of fuel element. Heating was accomplished by Nichrome wire in the

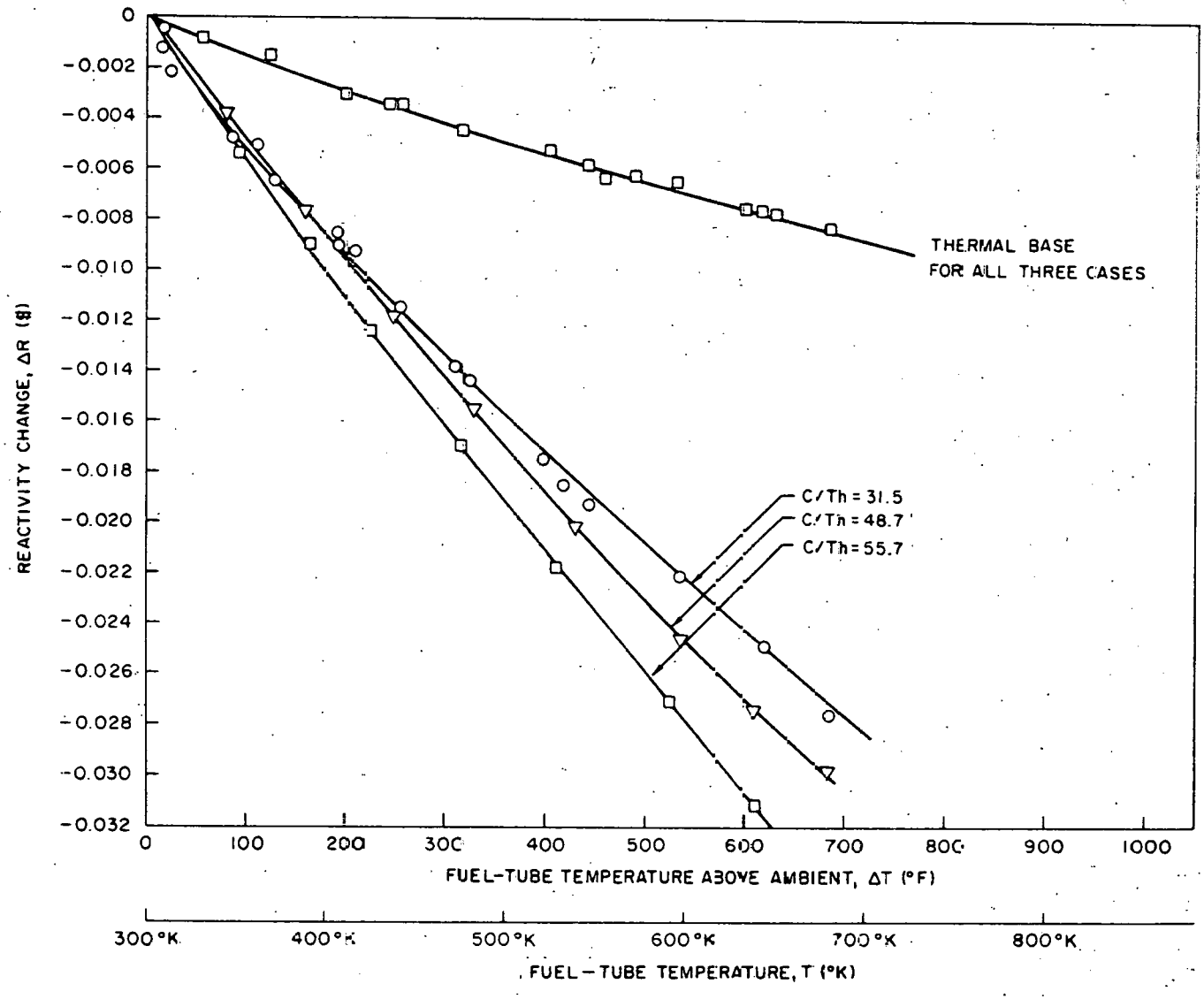


Fig. 10--Dependence of reactivity changes on temperature change, with a radially flat flux

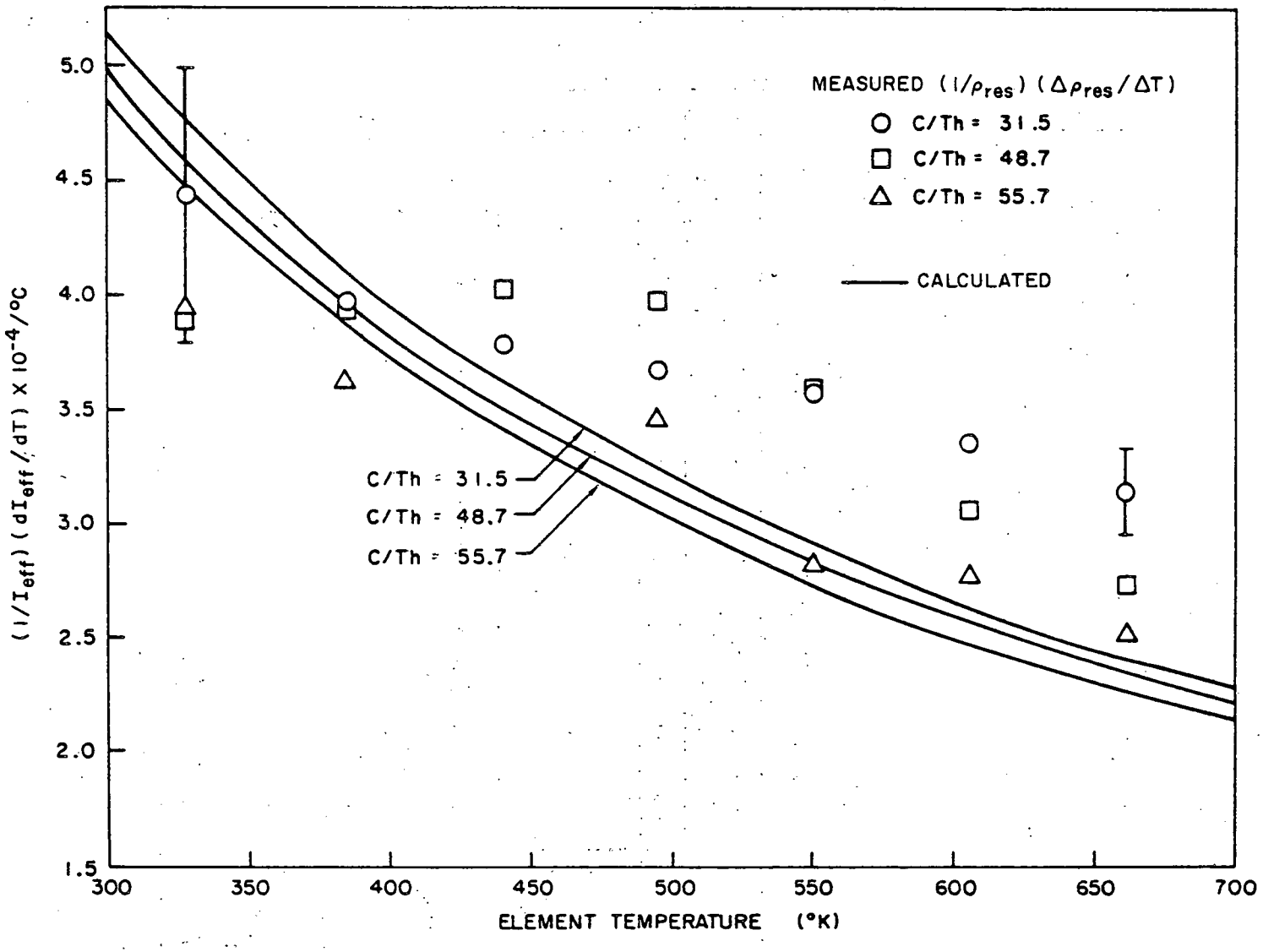


Fig. 11--Doppler coefficient for small HTGR annular fuel elements of several different C/Th ratios

Table III

DOPPLER COEFFICIENTS IN HTGR[a]

| C/Th Ratio | Measured Doppler Coefficients ($\times 10^{-4}/^{\circ}C$) | | Calculated Doppler Coefficients ($\times 10^{-4}/^{\circ}C$) |
|---|---|---|---|
| | Reactivity | Activation | |
| 31.5 | 3.70 | ---- | 3.39 |
| 48.7 | 3.61 | 3.70 | 3.28 |
| 53.7 | 3.26 | ---- | 3.17 |

[a] Average values for the temperature range $300^{\circ}$ to $700^{\circ}K$.

graphite sleeve. The oven was evacuated to a pressure below 20 $\mu$. The shell temperature was found to be 130°F with the oven operating at 1000°F. Internal thermocouples showed less than a 5°F variation from center to edge at a center temperature of 1000°F.

The activation technique used to measure the Doppler coefficient was based on activation of thorium and vanadium detectors in three positions, namely, in a fuel element heated in the oven, in a cool fuel element outside the oven, and in a Maxwellian spectrum. Gold-197 was activated in the latter two of these positions and used as the standard. The detectors exposed inside and outside the oven were placed at the same positions in their respective fuel elements. The Maxwellian flux was developed in the thermal column on the side of the TRIGA [8] reactor. The activation measurements in the Maxwellian flux made it possible to eliminate the counting-geometry factor. Measurements of the vanadium activation rates in the hot and cold samples made it possible to separate the change in thorium absorption rates arising from changes in the thermal-neutron absorption. By subtracting this component from the total changes in thorium absorption rate, the Doppler coefficient was obtained.

## V. CRITICAL-EXPERIMENT MEASUREMENTS IN THE CLEAN-GEOMETRY ASSEMBLY

The test-lattice experiments were directed primarily toward the development of fundamental information such as the evaluation of effective resonance integrals and Doppler coefficients for thorium in HTGR fuel compacts. In contrast, the experiments on the one-sixth-scale mock-up were designed to test the accuracy of the calculational procedures for clean, reflected reactors having a composition in the range of the HTGR. [3]

Table IV shows a comparison of the characteristics of the small-scale mock-up assembly and the Peach Bottom reactor. It can be seen from the $C/Th/U^{235}$ atom ratios for the two reactors that the critical assembly was more lightly loaded than the Peach Bottom reactor. The lighter loading and the greater effectiveness of the reflector in the critical assembly resulted in a much softer spectrum than was calculated for the Peach Bottom reactor, and consequently the experiment was not a good test of epithermal-reaction characteristics. On the other hand, the small core and strong reflectors resulted in strong variations in both the epithermal- and thermal-neutron spectra along radial and axial traverses. Hence, the experiment was a severe test of the multigroup, multidimensional diffusion-theory programs for calculating the multiplication constant and neutron-flux distributions.

The critical assembly corresponded roughly to the cold, clean, unrodded configuration of the Peach Bottom HTGR. The multiplication of the HTGR under the same conditions would be about $k_{eff} = 1.12$. The difference in multiplication constants was due primarily to the much larger leakage from the smaller critical-assembly core. In addition, there was no rhodium present in the critical assembly.

Table V shows the results of diffusion-theory calculations of the critical assembly using various calculational models. Included in the

Table IV

COMPARISON OF CHARACTERISTICS OF THE ONE-SIXTH-SCALE MOCK-UP ASSEMBLY AND THE PEACH BOTTOM HTGR

| | Peach Bottom | Critical Assembly |
|---|---|---|
| Core length, in. . . . . | 90 | 48 |
| Core diameter, in. . . . . | 109 | 58.7 |
| Core volume, liters . . . . | 14,000 | 2,130 |
| Reflector thickness, in. . | ~24 | 24 |
| $U^{235}$ inventory, kg . . . . | 220 | 19.7 |
| C/Th/$U^{235}$ atom ratio . . | 1,824/6.7/1 | 2,775/12/1 |
| Boron/$U^{235}$ weight ratio . | ~0.005 | ~0.003 |

Table V

RESULTS OF DIFFUSION-THEORY CALCULATIONS FOR CRITICAL ASSEMBLY AND PEACH BOTTOM REACTOR

| Calculational Model | | Eigenvalue, k | |
|---|---|---|---|
| No. of Dimensions | No. of Groups | Peach Bottom | Critical Assembly |
| 2 | 10 | 1.095 | 0.997 |
| 2 | 4 | 1.098 | 0.977 |
| 1 | 4 | 1.090 | 0.960 |

table are similar results for the Peach Bottom reactor. It can be seen that the critical-assembly results were very sensitive to both the number of energy groups and number of dimensions used in the calculations. In the first calculation four epithermal groups and six thermal groups were used in a two-dimensional R-Z diffusion-theory calculation. The epithermal-group constants were computed from the multigroup code GAM-1 [14] and the thermal-groups constants from the thermalization code GATHER-1.[15] The two-dimensional, 10-group diffusion-theory code GAMBLE [16] was used for the eigenvalue calculations. The calculated multiplication constant for the critical assembly differed from the measured value by 0.3% in k. The Peach Bottom multiplication refers to the beginning-of-life condition with the reactor at operating temperature and all control rods removed.

By using four energy groups, i.e., three epithermal and one thermal group, an error of 2.3% in k was introduced in the critical-experiment calculation. The Peach Bottom multiplication was only altered 0.3% by this change in group structure. This smaller discrepancy is ascribed to the larger core dimensions and the smaller importance of spatial variations in the neutron energy spectrum for the power reactor.

Using the one-dimensional code FEVER [17] and four energy groups, the total discrepancy was about 4.0% in k for the critical experiment, showing the importance of the geometric effects in the smaller reactor. A small difference existed in the Peach Bottom multiplication probably due to the manner in which loading non-uniformities in the axial direction were homogenized in the one-dimensional model.

In general, the results showed the importance of adequate energy and geometric detail in calculational methods used for small, reflector-dominated reactors. However, the calculations indicated that the one-dimensional, four-group calculational model could be used with some confidence in static calculations of the Peach Bottom-type reactors. However, in burnup calculations, where composition changes occur in both the radial and axial directions during fuel burnup, a two-dimensional model would be required.

Distributed reactivity coefficients of boron and $U^{235}$ were measured in the critical assembly and compared with calculated values. The results are shown in Table VI. The calculated values indicated errors of about 3% and 5% for boron and fuel, respectively. It would have been desirable to have a harder spectrum in order to test the epithermal cross section for $U^{235}$ more rigorously. The discrepancy in the calculations is probably too small to indicate a significant uncertainty in the cross section.

The spatial distribution of the neutron flux was measured by the activation of bare and cadmium-covered manganese foils and was also used as a basis for checking calculations. Figure 12 shows the calculated manganese absorption rate as a function of radius, indicated by the solid lines. The crosses indicate measurements along a vertical traverse in the central plane of the core, while the circles represent measurements along a horizontal traverse. The deviations between the calculations and measurements are due primarily to the slightly different radial distances to the side reflector in the two directions. In general, the agreement between the calculated and measured reaction rates was very satisfying in view of the important variation of the neutron energy spectrum with radius.

The over-all temperature coefficient of the mock-up assembly was also measured by heating the core and reflector uniformly in small steps up to $500^{\circ}F$, and measuring the reactivity change from room temperature at each step.

The temperature coefficient was calculated by evaluating the effective group cross sections at various temperatures within the range of interest, using the slowing-down code GAM-I and the thermalization code GATHER-1. The GATHER-I calculations incorporated the use of scattering kernels as given by the SUMMIT [18] code for carbon and oxygen at the various temperatures calculated. The criticality of the system at each temperature was obtained by use of the two-dimensional diffusion-theory code GAMBLE, in which four slowing-down and six thermal energy groups were used.

Table VI

COMPARISON OF MEASURED AND CALCULATED DISTRIBUTED REACTIVITY COEFFICIENTS

| | Measured | Calculated |
|---|---|---|
| Boron, $/gram . . . . . | 0.132 | 0.136 |
| $U^{235}$, $/gram . . . . . | 0.00190 | 0.00199 |

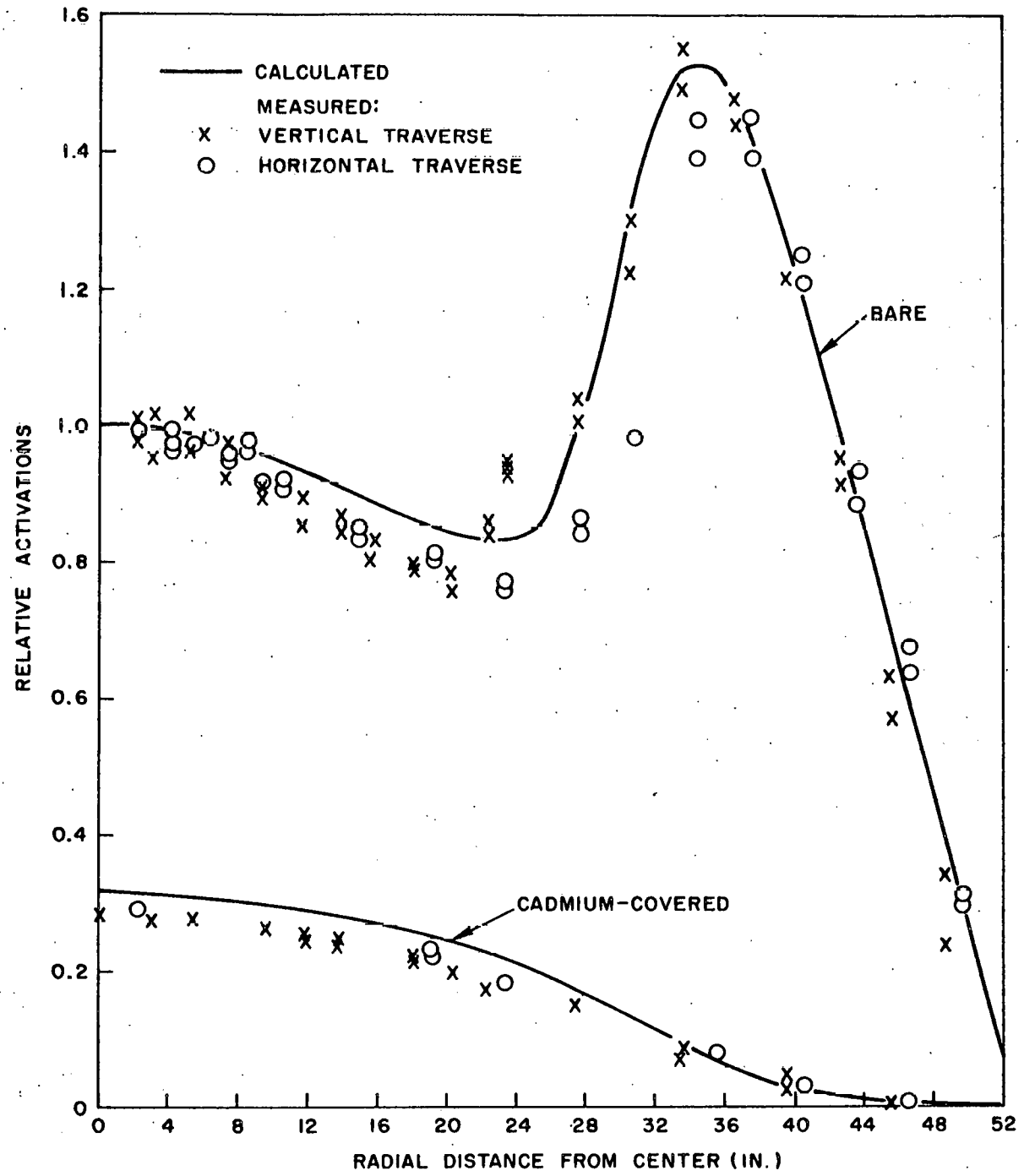


Fig. 12--Comparison of horizontal and vertical activation traverses for bare and cadmium-covered manganese foils, as calculated and as measured

The calculated multiplication of the system as a function of core temperature is compared with the multiplication measured with the assembly at various temperatures in Fig. 13. The calculated multiplication of the system is very close to the measured multiplication at all temperatures. The largest discrepancy occurred when the core was initially being heated. It is felt that the discrepancy in these initial values was produced by moisture which had been absorbed in the graphite before the assembly was constructed. During the process of heating the assembly, the moisture was driven off, and the discrepancy was nearly eliminated by the time a temperature of 350°F was reached.

At all temperatures, the Doppler coefficient was calculated to be the largest contributor to the over-all negative temperature coefficient, representing more than 90% of the net value. Other contributions arose from leakage effects, changes in thermal utilization, and changes in eta.

The results of the critical-experiment program on the small-scale mock-up assembly provided evidence that the calculational methods used in the analysis of the Peach Bottom reactor design are apparently adequate when properly applied.

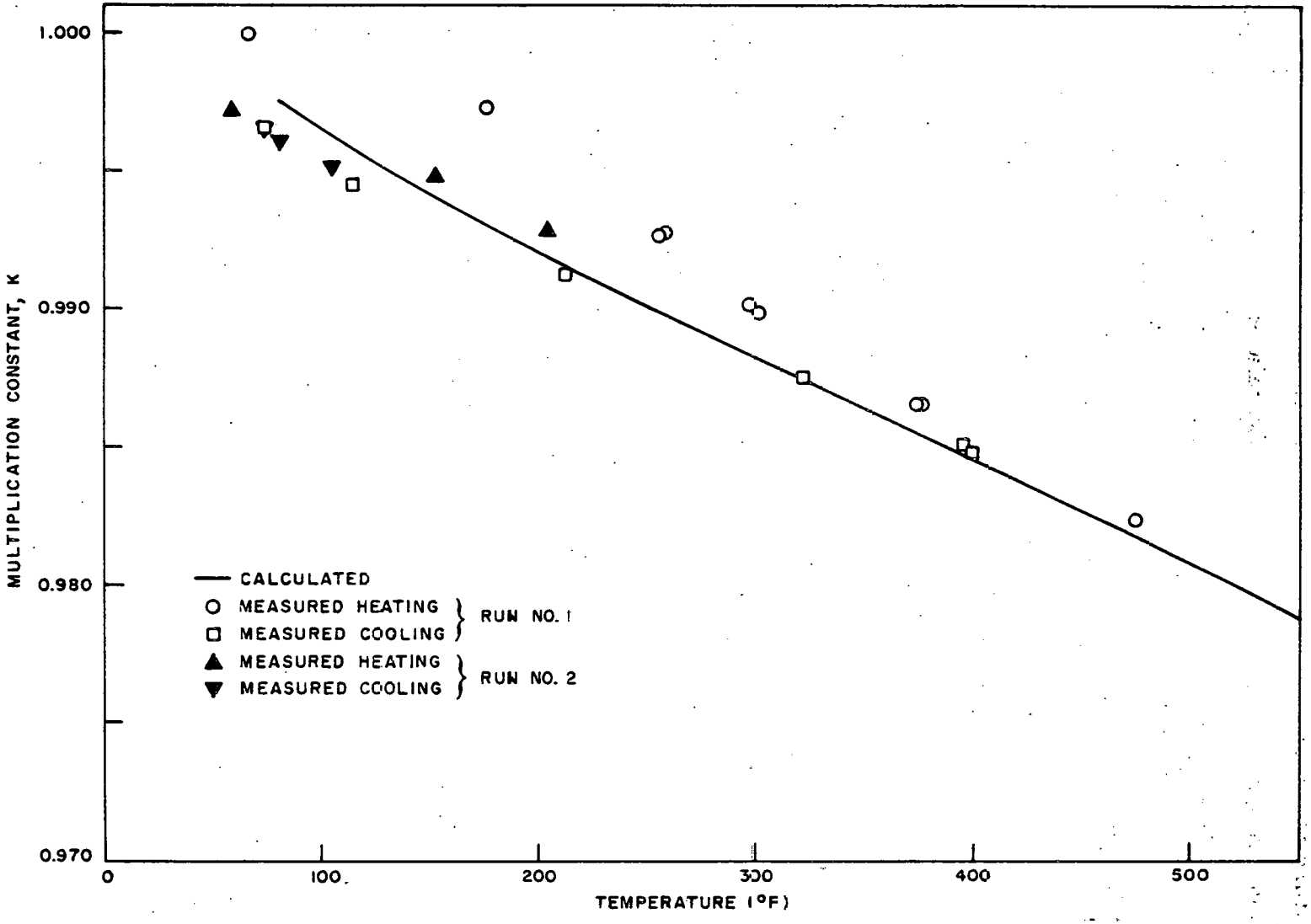


Fig. 13--Comparison of calculated and measured assembly multiplication constant as a function of core temperature

## REFERENCES


1. Pearce, R. M., "The Doppler Effect in Thermal Reactors," J. Nucl. Energy, Vol. A-13, 1961, p. 150.
2. Sampson, J. B., "Description of Peach Bottom HTGR Critical Assembly Loading with Central Exact Region," General Atomic Report GA-3539, October 25, 1962.
3. Brown, J. R., M. K. Drake, and K. R. Van Howe, "Correlation of Calculations and Experimental Measurements Made Using a Partial Core Mockup (Critical Assembly) of the Peach Bottom HTGR," General Atomic Report GA-3799, March 5, 1963.
4. Rosen, S. L., et al., CN(PNPL)-206, 1960.
5. Tattersall, R. B., et al., "Pile Oscillator Measurements of Resonance Absorption Integrals," J. Nucl. Energy, Vol. A-12, 1960, p. 32.
6. Macklin, R. L., and H. S. Pomerance, in Physics and Mathematics, Series I, McGraw-Hill Book Company,Inc., New York,1956, p. 186.
7. Drake, M. K., and J. R. Brown, "Experimental Techniques for Activation Measurement of Resonance Integrals," General Atomic Report GA-3125, January, 1963.
8. "TRIGA MARK I and MARK F Reactors and Supporting Facilities (Rev. A)," General Atomic Report GA-1695, March, 1961.
9. Sampson, J. B., "Analysis of Activation Measurements of Th-232 Resonance Captures in the Peach Bottom (40-MW(e) Prototype HTGR) Critical Assembly," General Atomic Report GA-3069, September, 1962.
10. Uttley, C. A., and R. H. Jones, in Atomic Energy Research Establishment Report AERE-PR/NP-2, 1962, p. 1; M. C. Mohon and C. M. Mycock, unpublished data.
11. Nordheim, L. W., private communication.

12. Sampson, J. B., and J. R. Brown, "Measured Doppler Coefficient of Thorium Dispersed in Graphite," General Atomic Report GA-3422, February, 1963.

13. Hurwitz, H., Jr., "Note on the Theory of Danger Coefficients," Knolls Atomic Power Laboratory Report KAPL-98, September, 1948.

14. Joanou, G. D., and J. S. Dudek, "GAM-I: A Consistent $P_1$ Multigroup Code for the Calculation of Fast Neutron Spectra and Multigroup Constants," General Atomic Report GA-1850, June, 1961.

15. General Atomic internal memorandum.

16. Dorsey, J. P., "GAMBLE: A Program for the Solution of the Multigroup Neutron-Diffusion Equations in Two Dimensions, With Arbitrary Group Scattering, for the IBM-7090 Fortran-II System," General Atomic Report GA-4246, June 15, 1963.

17. Todt, F., "FEVER: A One-Dimensional, Few Group Depletion Program for Reactor Analysis," General Atomic Report GA-2749, November, 1962.

18. Bell, J., "SUMMIT: An IBM-7090 Program for the Computation of Crystalline Scattering Kernels," General Atomic Report GA-2492, June, 1962.